Available online at www.sciencedirect.com
ScienceDirect
Journal of Solid State Chemistry 180 (2007) 2248–2255
JOURNAL OF SOLID STATE CHEMISTRY
www.elsevier.com/locate/jssc

Crystal structure and phase transitions of Sr_2CdWO_6

M. Gateshki[a], J.M. Igartua[b,*], A. Faik[b]

[a]*Australian Nuclear Science and Technology Organization, Private Mail Bag 1, Menai, NSW 2234, Australia*
[b]*Fisika Aplikatua II Saila, Zientzia eta Teknologia Fakultatea, Euskal Herriko Unibertsitatea, P.O. Box 644, Bilbao 48080, Spain*

Received 19 March 2007; received in revised form 24 May 2007; accepted 27 May 2007
Available online 3 June 2007

Abstract

The crystal structure of Sr_2CdWO_6, prepared by solid state reaction, was determined by high-resolution X-ray diffraction at different temperatures. At room temperature, this compound has a monoclinic structure (space group $P2_1/n$) with $a = 5.7463(1)$, $b = 5.8189(1)$, $c = 8.1465(1)$, $\beta = 90.071(1)$. At 1105 K the structure is converted to tetragonal (space group $I4/m$). Diffraction data also suggest that a cubic phase exists above 1220 K. Comparing the phase transition temperatures of Sr_2CdWO_6 with those of other compounds of the Sr_2MWO_6 family reported previously, it was observed that the transition temperatures are higher in compounds with low-tolerance factors. At the same time, the temperature range in which the intermediate tetragonal phase exists is reduced.

PACS: 61.10.Nz; 61.50.Ks; 61.66.Fu; 64.70.Kb

Keywords: Double perovskite; X-ray diffraction; Crystal structure; Phase transitions

1. Introduction

In recent years, the structural properties of double perovskite compounds with general formula $A_2BB'O_6$ have been extensively studied [1–3]. The double perovskite structure can be represented as a three-dimensional network of alternating BO_6 and $B'O_6$ octahedra, with A-atoms occupying the 12-coordinated interstitial spaces between the octahedra. The aristotype structure of this family is cubic [4] with the space group $Fm\bar{3}m$ (cubic, no. 225) [5]; however, due to a mismatch between the size of the A-site cation and the cuboctahedral space between the octahedra, many such materials undergo one [6], two [7] or even more [8] structural phase transitions at different temperatures. These structural transformations can be conveniently described as changes in the way the BO_6 and $B'O_6$ are rotated with respect to the crystallographic axes of the material to accommodate the size of the A-site cations [9,10]. In previous articles [11,12], we studied the structural phase transitions occurring in the materials with general formula Sr_2BWO_6 and B = Ni, Co, Zn, Ca, Mg. All of these materials undergo temperature-induced phase transitions with the following symmetry changes: $I4/m$ (tetragonal, no. 87) $\rightarrow Fm\bar{3}m$, for B = Ni, Mg; and $P2_1/n$ (monoclinic, no. 14, non-standard setting) $\rightarrow I4/m \rightarrow Fm\bar{3}m$, for B = Co, Zn, Ca. According to the Glazer classification [9] these distorted structures have the following tilt systems: $P2_1/n$, $a^+b^-b^-$; $I4/m$, $a^0a^0c^-$ and $a^0a^0a^0$ [4]. It was found that in materials with relatively small B-site cation (Ni,Mg,Zn,Co) the cubic aristotype structure is achieved at lower temperature than in the case of Sr_2CaWO_6 with larger B cation. In order to extend this study and establish a relation between the structural parameters of the materials and the temperature at which such transitions occur, in this article we report the crystal structures observed in Sr_2CdWO_6 at different temperatures, by means of synchrotron radiation powder diffraction study.

The first preparation of Sr_2CdWO_6 was reported in [13]. The room-temperature structure of Sr_2CdWO_6 was found to be of the ordered perovskite type, with the orthorhombic $Pmm2$ (no. 25) space group. This space group was chosen because of the piezoelectric properties observed in

*Corresponding author. Fax: +34 94 601 3500.
E-mail address: josu.igartua@ehu.es (J.M. Igartua).

0022-4596/$ - see front matter © 2007 Elsevier Inc. All rights reserved.
doi:10.1016/j.jssc.2007.05.022

Sr_2CdWO_6 by the author; although, no experimental results evidencing such properties were presented. The *Pmm*2 space group can accommodate the B cation ordering and the presence of a polar moment in the structure. The structure of Sr_2CdWO_6, presented in [13], was refined using conventional X-ray powder diffraction data. In this structure, the CdO_6 and WO_6 octahedra are deformed, but without any tilt or rotation. Also, the cations Cd^{2+} and W^{6+} were found to be displaced from the centers of their respective octahedra. Due to this structural determination, Sr_2CdWO_6 was included in the list of non-centrosymmetric oxides [14]. In another work [15], the room-temperature crystal structure of Sr_2CdWO_6 was referenced as tetragonal; however, no structural details were reported.

The study of Sr_2CdWO_6 at high temperatures, reported in [13], consists of DTA measurements and one structural determination at 1133 K. The DTA measurements showed a reversible thermal anomaly at about 1077 K; and the structure at 1133 K was refined with the $Fm\bar{3}m$ space group.

2. Experimental

2.1. Sample preparation

For the preparation of the sample, the standard method of solid-state chemical reaction was used. Stoichiometric amounts of the reacting compounds were mixed according to the following chemical reaction:

$$2SrCO_3 + CdO + WO_3 \rightarrow Sr_2CdWO_6 + 2CO_2 \uparrow .$$

The reacting compounds (all delivered by Sigma-Aldrich) had the following purities: $SrCO_3$(99.995%), WO_3(99.995%) and CdO(99.99%). All compounds were used as received. The starting materials were mixed and ground in an agate mortar; and subsequently heated in air in alumina crucibles. The following heat treatment was used: 24 h at 1120 K; 24 h at 1170 K; and 48 h at 1220 K. After each heating, the sample was cooled down slowly (3 K/min); and re-ground (re-mixed) to improve homogeneity. In order to control the quality of the obtained material, X-ray diffraction measurements were performed after each heating. Higher heating temperatures were also attempted, but we observed volatilization of Cd. This was deduced from the color of the material that changes form light gray to yellow and the progressive increase of the Sr_2WO_5 impurity in the sample as observed by X-ray diffraction. The X-ray studies also showed that the diffraction lines of Sr_2CdWO_6 are broader compared to those of the other members of the Sr_2MWO_6 family studied previously [11,12]. This is probably due to the fact that the synthesis temperature was lower, and such lower temperature can give as a result crystalline grains with smaller sizes.

Small amounts ($\approx$ 1.7% weight fraction) of the impurity $SrWO_4$ was found in the final material: this impurity was included as a known additional phase in the Rietveld refinements of the structure of the studied compound. $SrWO_4$ has symmetry $I4_1/a$. Known structural parameters from the literature [16] were used; and these were not refined.

2.2. X-ray powder diffraction measurements

Two different sets of diffraction experiments were performed with the studied sample. First, in order to establish the presence of phase transitions and their temperatures, X-ray data were collected in the 2θ interval from 71.5 to 73.5, with a temperature step of 15 K. This was done using a Philips X′Pert MPD System with CuK_α (Ni filter) radiation, equipped with a proportional detector and an Anton Paar HTK16 temperature chamber, with a temperature stability of 0.5 K. Intensity data were collected using Bragg–Brentano parafocusing geometry and 12 s counting time at each step.

Second, for structural determination and refinement of Sr_2CdWO_6, high-resolution X-ray diffraction experiments at selected temperatures (300, 770, 1120 K) were performed using the X7A beam-line at the National Synchrotron Light Source (Brookhaven National Laboratory) [17]. The radiation wavelength was 0.8005 Å. It was obtained using a Si(1 1 1) monochromator; and was calibrated with a CeO_2 standard sample. Diffracted radiation was collected by a linear position sensitive detector mounted on the 2θ arm of the diffractometer, at a distance of 1 m from the sample. In this case, the sample was placed in a quartz capillary and rotated during the experiment to reduce preferred-orientation effects.

The Rietveld refinement of the structures was performed with the FullProf program [18].

3. Results and discussion

At all temperatures covered, the 2θ region chosen (71.5–73.5) for the phase transition search contains a group of diffraction peaks that has been identified as especially sensitive to the structural changes occurring in double perovskite materials [12]. This experiment showed that the only changes that can be interpreted as indications of phase transitions are the appearance of a shoulder on the low-angle side of the peak, at 1105 K (Fig. 1); and the subsequent unification of this shoulder with the main peak, occurring at about 1220 K. This behavior is very similar to that observed in Sr_2CaWO_6 [12], where these changes were interpreted as evidences of the material undergoing two phase transitions; first, from monoclinic structure to tetragonal one, and (at higher temperature) from tetragonal to cubic. To clarify the structural changes occurring in Sr_2CdWO_6, high-resolution diffraction measurements using synchrotron radiation were performed at three different temperatures: 300, 770 and 1120 K. It was not possible to reach higher temperatures due to instrument limitations.

The diffraction pattern collected at 300 K is shown in Fig. 2. The attempt to refine the structure of Sr_2CdWO_6

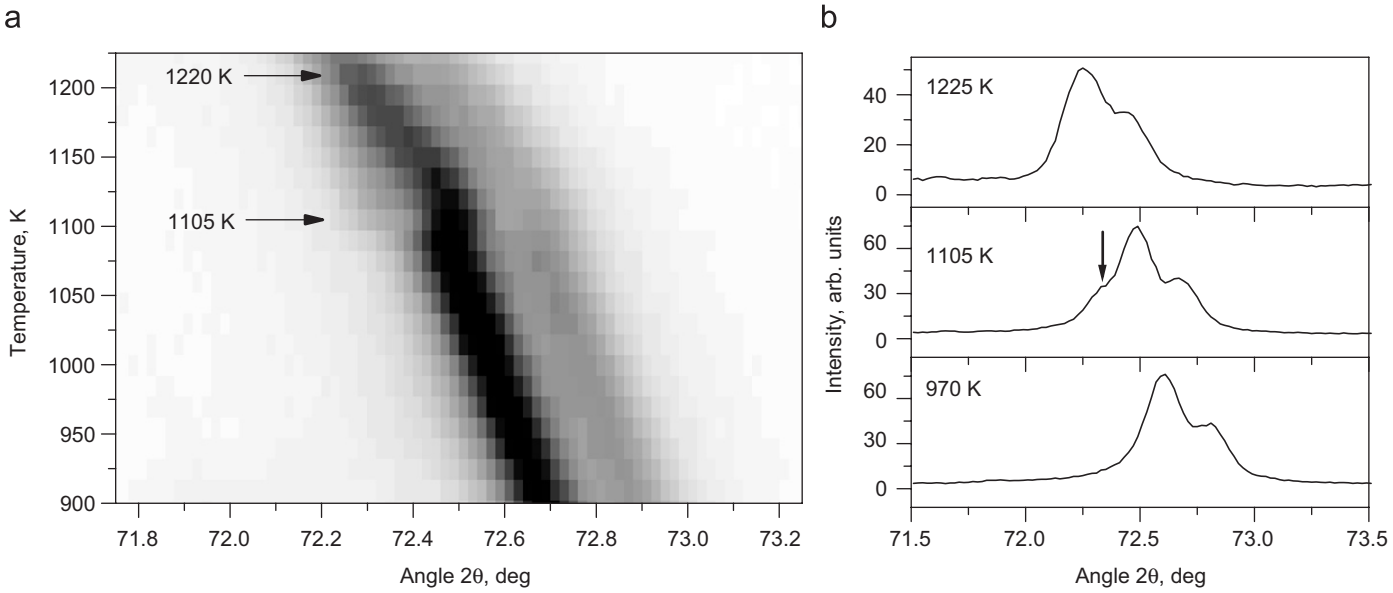

Fig. 1. Temperature evolution of the (620) cubic reflection of Sr_2CdWO_6. In (a), scattered intensity is represented with shades of gray—black corresponds to high intensity and white to low intensity. The tetragonal splitting existing in the temperature range from 1105 to about 1220 K can be observed. The shoulder appearing at 1105 K is marked with an arrow in (b).

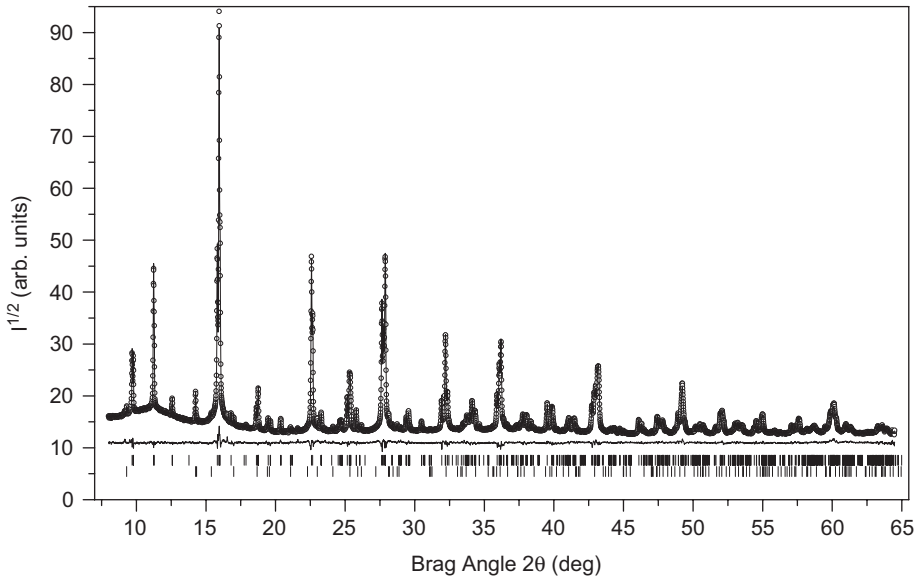

Fig. 2. Experimental (symbols) and calculated (line) powder diffraction profiles for the Rietveld refinement of Sr_2CdWO_6 at room temperature using a structural model with $P2_1/n$ space group. The bars in the lower part of the graphics represent the Bragg peak positions of the main phase and the $SrWO_4$ impurity (lower set of bars).

using a structural model with the *Pmm*2 space group, as suggested previously [13], gave a reasonably good fit of the diffraction profile: no unindexed lines or large differences between the experimental and calculated intensities were observed. However, many fine details in the pattern were not well accounted for by the model. These problems were successfully solved by performing a refinement based on the monoclinic structure with space group $P2_1/n$ observed in many double perovskite compounds [19–22], including several compounds with the general formula Sr_2MWO_6 [11,12,23]. One example of a diffraction reflection where the monoclinic model gives improvement, is shown in Fig. 3. The peak located at higher 2θ angle is considerably broader than the peak at lower angle, also shown in the figure. This difference in the widths of the two peaks can be easily explained as a result of a monoclinic distortion of the unit cell, while the orthorhombic structural model is not able to reproduce this experimental observation. The better visual fit of the experimental data with the $P2_1/n$ model is accompanied, also, with significant

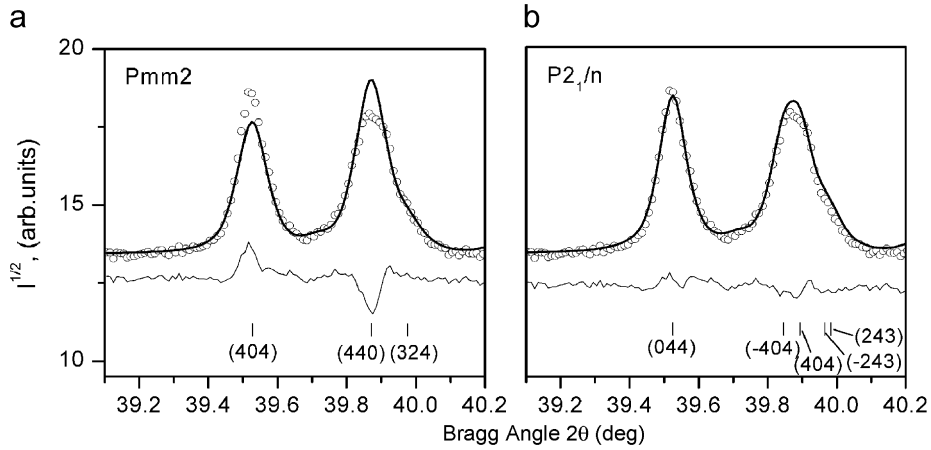

Fig. 3. Experimental diffraction data for Sr_2CdWO_6 at 300 K (symbols) compared with the diffraction patterns calculated after refinement (lines) using structural models with symmetries *Pmm*2 (a) and $P2_1/n$ (b). Only the monoclinic model reproduces correctly the diffraction intensities observed in the experiment.

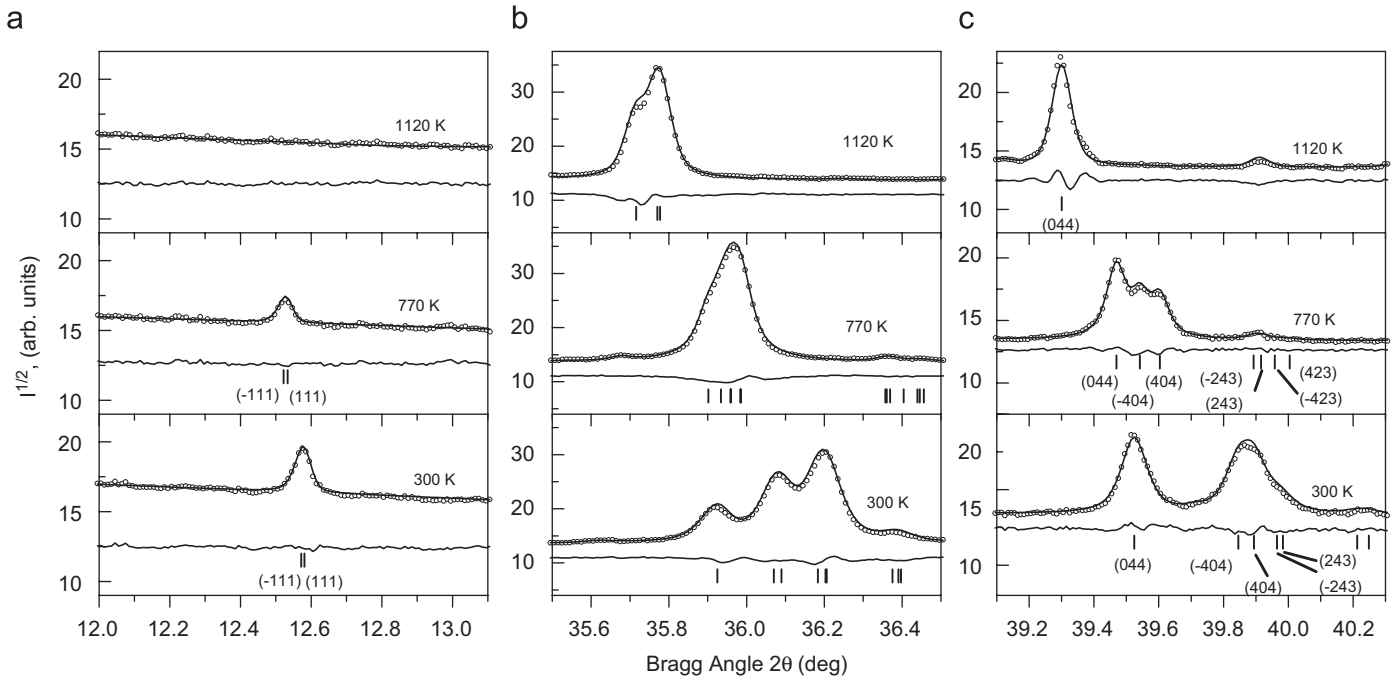

Fig. 4. Temperature evolution of three groups of diffraction peaks located at different 2θ positions. The calculated and difference diffraction profiles (lines) are obtained after Rietveld refinement of the structure at each temperature. The structural models used in the refinement have the following symmetries: $P2_1/n$ for 300 and 770 K, and $I4/m$ for 1120 K. For clarity, only the Bragg positions of the main phase are shown as bars in the lower part of the graphics.

improvement in the agreement factors of the refinement. In the diffraction data collected at 770 K, the presence of the monoclinic distortion is even clearer. There is a visible splitting (middle panel of Fig. 4c) of the peak, caused by the difference in 2θ positions of the (−404) and (404) reflections. The structural details of Sr_2CdWO_6 at room temperature and 770 K, refined by assuming monoclinic lattice and the $P2_1/n$ space group, are shown in Table 1.

With respect to the piezoelectric properties observed for Sr_2CdWO_6 in [13], it should be pointed out that a structure with the $P2_1/n$ space group, which is centrosymmetric, cannot present such properties. If the crystal structure had a symmetry described by some of the non-centrosymmetric subgroups of $P2_1/n$: $P2_1$, Pn or $P1$, additional diffraction peaks should be observed, since these space groups have different extinction conditions. Such additional peaks could not be observed in our diffraction data, and it was not possible, on the base of the collected X-ray powder diffraction data, to confirm that Sr_2CdWO_6 is non-centrosymmetric.

Before analyzing the structure of Sr_2CdWO_6 at 1120 K, it should be noted that the diffraction experiment at this

Table 1
Crystal structure data and refinement results for Sr_2CdWO_6 at 300, 770 and 1120 K

Temperature space group Agreement factors	Lattice parameters (Å)	Atom	Wyck. pos.	x	y	z	B_{iso}(Å^2)
300 K	$a = 5.7463(1)$	W	2a	0	0	0	0.5(1)
$P2_1/n$	$b = 5.8189(1)$	Cd	2b	1/2	1/2	0	0.7(1)
$R_{wp} = 7.18\%$	$c = 8.1465(1)$	Sr	4e	0.0081(7)	0.5375(1)	0.2508(3)	0.9(1)
$R_B = 4.29\%$	$\beta = 90.071°(1)$	O_1	4e	0.089(1)	0.021(2)	−0.23(1)	2.7(1)
$\chi^2 = 11.6$		O_2	4e	0.254(2)	−0.194(2)	0.032(2)	2.7(1)
		O_3	4e	0.182(2)	0.250(2)	0.058(2)	2.7(1)
773 K	$a = 5.7905(1)$	W	2a	0	0	0	0.7(1)
$P2_1/n$	$b = 5.8122(1)$	Cd	2b	1/2	1/2	0	1.2(1)
$R_{wp} = 7.19\%$	$c = 8.1974(1)$	Sr	4e	0.0050(1)	0.5261(3)	0.2512(5)	1.8(1)
$R_B = 4.06\%$	$\beta = 90.091°(1)$	O_1	4e	0.073(3)	0.024(2)	−0.216(2)	3.9(1)
$\chi^2 = 9.86$		O_2	4e	0.282(2)	−0.203(2)	0.009(3)	3.9(1)
		O_3	4e	0.179(3)	0.264(3)	0.046(2)	3.9(1)
1120 K	$a = 5.8273(1)$	W	2a	0	0	0	1.5(1)
$I4/m$	$c = 8.2564(1)$	Cd	2b	0	0	1/2	2.2(1)
$R_{wp} = 8.02\%$		Sr	4d	0	1/2	1/4	3.4(1)
$R_B = 4.5\%$		O_1	4e	0	0	0.230(2)	6.1(1)
$\chi^2 = 14.1$		O_2	8h	0.265(2)	0.181(3)	0	6.1(1)

The atomic positions (in fractional coordinates) and isotropic atomic displacement parameters were refined in the space groups $P2_1/n$ (300 K and 770 K) and $I/4m$ (1120 K).

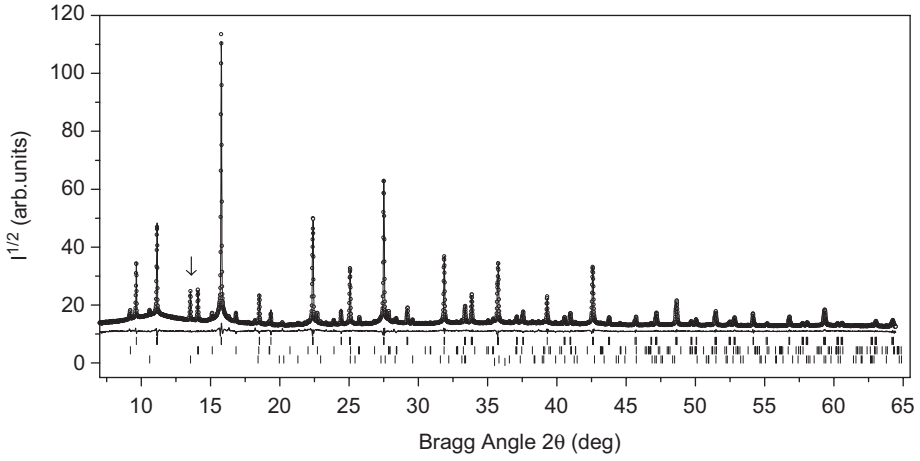

Fig. 5. Experimental (symbols) and calculated (line) powder diffraction profiles for the Rietveld refinement of Sr_2CdWO_6 at 1120 K using a structural model with $I4/m$ space group. The bars in the lower part of the graphic represent the Bragg peak positions of the main phase, the $SrWO_4$ impurity (middle set of bars) and SiO_2 (lower set of bars). The arrow points to the most intense diffraction peak of SiO_2.

temperature (Fig. 5) shows that the weight fraction of $SrWO_4$ increases to about 4%, indicating partial decomposition of the sample. Also, at this temperature, several low-intensity peaks appear that are incompatible with the perovskite structure. Through search–match procedure, these peaks were identified as originating from quartz, and are probably due to crystallization process in the material of the capillary tube.

Regarding the Sr_2CdWO_6 material under study, there are several important observations that can help identify its structural type at 1120 K. For example, all diffraction peaks with indices of the type $h + k + l = 2n + 1$ present at lower temperatures are missing at 1120 K (see Fig. 4a). This shows that there is a change from a primitive unit cell to a body-centered one. Also, while some of the peaks remain split (Fig. 4b) at this temperature, others are well represented by a single diffraction reflection (Fig. 4c). Analyzing the peak splitting, it becomes clear that at 1120 K the unit cell is tetragonal.

If this result is compared with the list of the possible double perovskite structures suggested by group-theoretical analysis [10,11], it can be assumed that at 1120 K Sr_2CdWO_6 has the symmetry $I4/m$ (tilt $a^0a^0c^-$). The pattern calculated using this symmetry accounts for all important features of the experiment (Fig. 5) and provides reasonably good agreement factors. Structural details for

Sr_2CdWO_6 at 1120 K are given in Table 1. It can be seen that the isotropic atomic displacements of the oxygen atoms are rather large even considering that the experiment is performed at high temperature. Refinement of the structure was attempted also with the space group $I4$ which allows not only octahedral rotations but also atomic displacements along the c-axis. This did not lead to any improvement of the agreement factors despite the increased number of refinable atomic coordinates. One likely cause for the unusually large isotropic displacements of the oxygen atoms is the modified chemical composition of the material due to the ongoing decomposition process.

The tetragonal distortion of the unit cell at 1105 K is also responsible for the peak splitting observed in Fig. 1. As already mentioned, this splitting gradually disappears at higher temperature (upper panel of Fig. 1b), and suggests that at a temperature of about 1220 K the unit cell is converted to cubic. This cubic phase most probably has the symmetry of the aristotype double perovskite structure with space group $Fm\bar{3}m$. It was not possible to confirm this hypothesis through structural refinement, due to the instrumental limitations, and to the fact that at this temperature the decomposition process accelerates (note the diminished intensity of the peak shown in the upper panel of Fig. 1b, compared to the other two temperatures). Further studies are required to confirm the presence of the cubic phase at high temperatures and to establish its symmetry.

The structural analysis based on the presented temperature-dependent high-resolution diffraction experiments suggests that the phase transition sequence existing in Sr_2CdWO_6 is $P2_1/n \rightarrow I4/m \rightarrow Fm\bar{3}m$; being the first transition discontinuous, and the second one continuous. The same sequence is known to exist in many other double perovskites [24], including Sr_2BWO_6 (B = Co, Zn, Ca) [11,12], suggesting that the temperature evolution of their structures is governed by the same principles. It is usually assumed [24] that the driving force of the structural changes in this kind of materials is the mismatch between the size of the A cation (Sr^{2+} in this case) and the interstitial space between the BO_6 and $B'O_6$ octahedra. This mismatch is measured by means of the so-called tolerance factor [25]:

$$t = \frac{d_{A-O}}{\frac{1}{\sqrt{2}}(d_{B-O} + d_{B'-O})}.$$

The mean d_{A-O}, d_{B-O} and $d_{B'-O}$ bond lengths can be obtained from tables of ionic radii [26] or by calculating the distances that give the nominal oxidation states of the cations in the bond–valence method [27,28]. Fig. 6 shows the phase transition temperatures as a function of the tolerance factor t, calculated using the second method. As the figure shows, the phase transition temperatures increase at lower values of t. Also, the temperature range in which the tetragonal phase exists is narrower at low t. These results are very similar to those observed in Rb_2KBF_6 (B = Sc, In, Lu, Er, Ho) elpasolites [29], and confirm that the most important factor governing the appearance of octahedral tilts in the double perovskite structure and the temperature range in which they exist is the mismatch between the size of the A cation and interstitial space between the BO_6 and $B'O_6$ octahedra. There is one exception, however, and this is the case of Sr_2MgWO_6. This compound has a tolerance factor that is very close to that of Sr_2CoWO_6 but considerably lower temperature of the cubic-to-tetragonal transition. Also, the low-temperature studies of this compound [12] showed that the tetragonal structure is preserved at least down to 26 K, while in Sr_2CoWO_6 the monoclinic phase is observed below 250 K [11,23]. This suggests that other factors can also influence the phase transition temperatures. Such factors could be the presence of oxygen or cation vacancies, and the electronic properties of the particular cations. If the lattice parameters of Sr_2MgWO_6 [12] are compared with those obtained in other recent studies, [30–32] using also different precursor materials and synthesis temperatures, it can be seen that they are within 0.1% of each other. This makes unlikely the presence of excessive amount of vacancies in our sample and also any other synthesis related effect. The temperature of the tetragonal-cubic phase transition reported in [30] is identical (570 K) to the one observed in our previous study. Similarly, low-temperature studies of Sr_2MgWO_6 [32] show that the tetragonal phase is retained down to 15 K. Further studies are required to establish the reason for Sr_2MgWO_6 not following the general trend observed in Fig. 6.

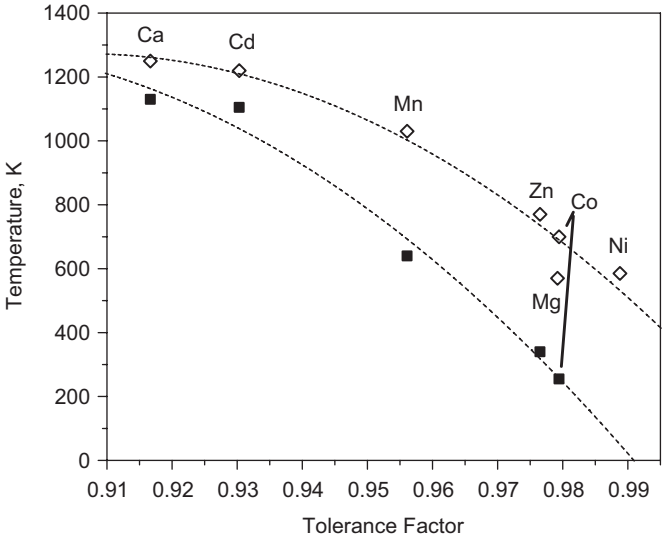

Fig. 6. Phase transition temperatures of Sr_2MWO_6 compounds, as a function of their tolerance factors. The temperature values used were taken from previously reported studies: [12], for M = Ca, Mg; and [11], for M = Zn, Co, Ni. The phase transition temperatures for M = Mn are based on results obtained from high-temperature XRD that will be published elsewhere. Open diamonds represent the tetragonal-cubic transition, and solid squares represent the monoclinic-tetragonal transition (if existing) in each compound. Lines are guides to the eye.

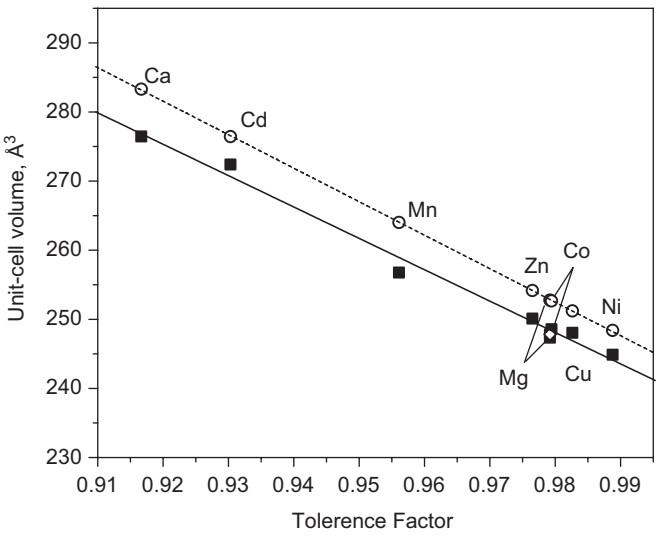

Fig. 7. Variation of the unit-cell volumes at ambient temperature of Sr_2MWO_6 compounds, as a function of the tolerance factor. Both the experimental values (solid squares) and those calculated with the program SPuDS (open circles) show linear dependence with the same slope. The unit-cell volume of Sr_2MgWO_6, obtained from the structural data given in the work by Khalyavin et al. [31], is also included as a reference (open diamond).

If the unit cell volumes at ambient temperature of the studied double perovskite oxides is plotted as a function of the tolerance factor (Fig. 7), a linear dependence can be observed. This, again, reinforces the result that structural properties of double perovskites are predetermined by the cationic radii. On the same figure the unit cell volumes calculated for the studied compounds using the program SPuDS (Version 2—Creation date December 2005) [19,33] are given. For each compound the tilt pattern observed in the experiment was used in the calculation. The calculated values have a linear dependence on the tolerance factor with the same slope observed in the experiment. The only difference is that the calculated values slightly overestimate the unit cell volumes for all compounds.

4. Conclusions

At ambient temperature, the crystal structure of Sr_2CdWO_6 was found to be monoclinic with the space group $P2_1/n$, which is different from the previously reported orthorhombic ($Pmm2$) structure. Sr_2CdWO_6 undergoes a phase transition at 1105 K above which the structure becomes tetragonal ($I4/m$). The high-temperature diffraction data also suggest that there is another phase transition at around 1220 K, which transforms the structure to cubic. The mechanism of these phase transitions is related to the mismatch of the size of the A cation and the cuboctahedral space between the WO_6 and CdO_6 octahedra. The bigger size of the Cd^{2+} cation, with respect to that of some other members of the Sr_2MWO_6 family, such as Co^{2+} and Ni^{2+} cations, for instance, leads to a structure with lower symmetry at room temperature. When the phase transition temperatures of Sr_2CdWO_6 are compared with those of other compounds of the Sr_2MWO_6 family reported previously, it becomes clear that the transition temperatures increase at low-tolerance factors, and, that, at the same time, the temperature range in which the intermediate tetragonal phase exists is reduced. This comparison also showed that the temperature-dependent structural evolution of the Sr_2MgWO_6 compound considerably deviates from the general trend observed in the rest of the Sr_2MWO_6 materials.

Acknowledgments

Part of this work was carried out at the National Synchrotron Light Source (X7A beam-line), Brookhaven National Laboratory (BNL), which is supported by the U.S. Department of Energy, Division of Material Sciences and Division of Chemical Sciences. The authors thank to Dr. T. Vogt and Dr. B. Noheda from BNL for their kind and precise assistance during the experiments. This work was done in part under project numbers: UPV 0063.310-13564/2001-2006 and FIS2005-07090. The authors thank the technician of SGIker, Dr. J.P. Chapman, financed by the Programa Nacional de Potenciación de Recursos Humanos del Plan Nacional de Investigación Científica, Desarrollo e Innovación-Ministerio de Ciencia y Tecnología y Fondo Social Europeo (FSE), for the X-ray diffraction experiments.

References

[1] K.-I. Kobayashi, T. Kimura, H. Sawada, K. Terakura, Y. Tokura, Nature 395 (1998) 677–680.
[2] M. DeMarco, H.A. Blackstead, J.D. Dow, M.K. Wu, D.Y. Chen, E.Z. Chien, H. Haka, S. Toorongian, J. Fridmann, Phys. Rev. B 62 (2000) 14301–14303.
[3] Y. Todate, J. Phys. Chem. Solids B 60 (1999) 1173.
[4] P.M. Woodward, Acta Cryst. B 53 (1997) 32.
[5] T. Hahn (Ed.), International Tables for Crystallography, vol. A, Kluwer, Dordrecht, 2002.
[6] O. Chmaissem, R. Kruk, B. Dabrowski, D.E. Brown, X. Xiong, S. Kolesnik, J.D. Jorgensen, C.W. Kimball, Phys. Rev. B 62 (2000) 14197.
[7] K. Yamamura, M. Wakeshima, Y. Hinatsu, J. Solid State Chem. 179 (2006) 605–612.
[8] L.O. Martin, J.P. Chapman, E. Hernndez-Bocanegra, M. Insausti, M.I. Arriortua, T. Rojo, J. Phys.: Condens. Matter 16 (2004) 3879–3888.
[9] A.M. Glazer, Acta Cryst. B 28 (1972) 3384;
A.M. Glazer, Acta Cryst. A 31 (1975) 756–762.
[10] C.J. Howard, B.J. Kennedy, P.M. Woodward, Acta Cryst. B 59 (2003) 463–471.
[11] M. Gateshki, J.M. Igartua, E. Hernández-Bocanegra, J. Phys.: Condens. Matter 15 (2003) 6199–6217.
[12] M. Gateshki, J.M. Igartua, J. Phys.: Condens. Matter 16 (2004) 6639–6649.
[13] Z. Fu, Sci. China A 34 (1991) 455.
[14] P. Shiv Halasyamani, K.R. Poeppelmeier, Chem. Mater. 10 (1998) 2753.
[15] M.D. Wei, Y. Teraoka, S. Kagawa, Mater. Res. Bull. 35 (2000) 521–530.

[16] E. Guermen, E. Daniels, J.S. King, J. Chem. Phys. 55 (1971) 1093–1097.
[17] ⟨http://www.nsls.bnl.gov/beamlines/beamline.asp?blid=X7A⟩.
[18] J. Rodríguez-Carvajal, Physica B 192 (1993) 55–69.
[19] M.W. Lufaso, P.W. Barnes, P.M. Woodward, Acta Cryst. B 62 (2006) 397–410.
[20] Q. Zhou, B.J. Kennedy, C.J. Howard, M.M. Elcombe, A.J. Studer, Chem. Mater. 17 (21) (2005) 5357–5365.
[21] Q. Zhou, B.J. Kennedy, M.M. Elcombe, Phys. B: Condens. Matter 385–386 (2006) 190–192.
[22] J.J. Blanco, M. Insausti, L. Lezama, J.P. Chapman, I. Gil De Muro, T. Rojo, J. Solid State Chem. 177 (2004) 2749–2755.
[23] M.C. Viola, M.J. Martínez-Lope, J.A. Alonso, J.L. Martínez, J.M. De Paoli, S. Pagola, J.C. Pedregosa, M.T. Fernández-Díaz, R.E. Carbonio, Chem. Mater. 15 (2003) 1655–1663.
[24] R.H. Mitchell, Perovskites. Modern and Ancient, Almaz Press, 2002.
[25] V.M. Goldschmidt, Str. Nor. Vidensk-Akad. Oslo 1 (1926) 1.
[26] R.D. Shannon, Acta Cryst. A 32 (1976) 751.
[27] N.E. Brese, M. O'Keeffe, Acta Cryst. B 47 (1991) 192–197.
[28] Accumulated Table of Bond Valence Parameters Version 2.2 Prepared by I.D. Brown, McMaster University, Hamilton, Ontario, Canada. Available at ⟨www.ccp14.ac.uk/ccp/web-mirrors/i_d_brown⟩.
[29] I.N. Flerov, M.V. Gorev, V.N. Voronov, Phys. Solid State 38 (1996) 396–401.
[30] S.J. Patwe, S.N. Achary, M.D. Mathews, A.K. Tyagi, J. Alloys Compds. 390 (2005) 396–401.
[31] D.D. Khalyavin, A.M.R. Senos, P.Q. Mantas, Powder Diff. 19 (2004) 280–283.
[32] S.N. Achary, K.R. Chakraborty, S.J. Patwe, A.B. Shinde, P.S.R. Krishnaa, A.K. Tyagi, Mater. Res. Bull. 41 (2006) 674–682.
[33] M.W. Lufaso, P.M. Woodward, Acta Cryst. B 57 (2001) 725–738.